Journal of Volcanology and Geothermal Research 310 (2016) 89–97

Contents lists available at ScienceDirect

Journal of Volcanology and Geothermal Research

journal homepage: www.elsevier.com/locate/jvolgeores

Timing of the Late Cretaceous ignimbrite flare-up at the eastern margin of the Eurasian Plate: New zircon U–Pb ages from the Aioi–Arima–Koto region of SW Japan

Daisuke Sato *, Hirohisa Matsuura, Takahiro Yamamoto

Geological Survey of Japan (GSJ), AIST, Central 7, 1-1-1 Higashi, Tsukuba, Ibaraki 305-8567, Japan

ARTICLE INFO

Article history:
Received 8 June 2015
Accepted 14 November 2015
Available online 11 December 2015

Keywords:
Aioi Group
Arima Group
Koto Rhyolites
U–Pb age
Cretaceous
Caldera

ABSTRACT

The Kinki district in the Inner Zone of southwest Japan is characterized by Late Cretaceous volcanic rocks of the Aioi and Arima groups and the Koto Rhyolites (from west to east). These rocks are dominated by pyroclastic flow deposits related to caldera-forming events. Here, we present new laser ablation–inductively coupled plasma–mass spectrometry (LA–ICP–MS) zircon U–Pb ages for the Aioi Group (four isolated caldera-filling deposits); the lower, middle, and upper parts of the Arima Group and one intrusive rock (the Kashihara Quartz Gabbro); and the lower and upper parts of the Koto Rhyolites, including the oldest volcanic unit within these rhyolites. These analyses yielded ages of ca. 86–82 Ma for the Aioi Group, ca. 83–81 Ma for the Arima Group, 78.6 Ma for the Kashihara Quartz Gabbro, and ca. 74–73 Ma for the Koto Rhyolites. The Aioi Group represents a cluster of calderas and the ages obtained for individual units in this group differ from the ages of adjacent units. The Arima Group and the Koto Rhyolites both consist of pyroclastic flow deposits associated with caldera-forming events, and the ages of these rocks are all the same within error. This suggests that the Aioi Group represents a series of individual caldera-forming eruptions that are distinct from the Arima Group and the Koto Rhyolites, which formed during a single stage of caldera formation. The U–Pb ages presented here indicate that the Late Cretaceous caldera-forming eruptions in the study area occurred at intervals of >1 Myr and represent individual events that lasted for <1 Myr. The oldest volcanic unit within the Kinki district is similar in age to the oldest volcanic unit within the Chubu district, suggesting that caldera-forming eruptions in southwest Japan commenced at ca. 90 Ma.

1. Introduction

Cretaceous igneous rocks are widespread throughout the Inner Zone of southwest Japan (Fig. 1). This zone represents a huge igneous belt that developed along the continental margin of East Asia before the Miocene opening of the Japan Sea (e.g., Takahashi, 1983). Early Cretaceous magmatism in southwest Japan is characterized by the intrusion of small volumes of high-Mg and adakitic magmas, and I-type granite magmas (e.g., Kamei et al., 2004). Kiji et al. (2000) and Kamei et al. (2004) suggested that some of the high-Mg and adakitic magmatism in this area was region to partial melting of subducted oceanic crustal and sedimentary material. The Late Cretaceous magmatism in this area is characterized by widespread silicic magmatism in the form of I-type granites and caldera-forming ignimbrites. Although the total volume of these ignimbrites is not known, this group includes the Nohi Rhyolite (Fig. 1), which is estimated to have a total volume of 5000–7000 km^3 (Yamada and Koido, 2005). Late Cretaceous volcanic rocks are dominantly pyroclastic flow deposits related to caldera-forming events (e.g., Nishikawa et al., 1983; Ozaki and Matsuura, 1988; Yamamoto, 2003). Determining the spatial and temporal variations in this Cretaceous magmatism requires precise geochronological and geological data. Precise U–Pb and chemical Th–U–total Pb isochron (CHIME) ages for I-type, high-Mg, and adakitic granitoids in this area have been reported recently (e.g., Suzuki and Adachi, 1998; Sakashima et al., 2003), indicating that this magmatism commenced at ca. 110–105 Ma. Volcanic rocks in southwest Japan have been dated at ca. 95–60 Ma by K–Ar and Rb–Sr isochron and fission-track (FT) methods, although some of these ages have been thermally reset, disagree with other ages, and are imprecise, with errors of several million years (e.g., Sawada and Itaya, 1993; Matsuura et al., 1995), meaning that the magmatic history of individual volcanic units is difficult to discern.

It is important to understand the timing of the Late Cretaceous ignimbrite flare-up in the study area in order to constrain the shift from high-Mg and adakitic volcanism with subduction of oceanic crustal material at the start of Early Cretaceous, to widespread I-type volcanism due to cooling oceanic crust. Here, we report new laser ablation–inductively coupled plasma–mass spectrometry (LA–ICP–MS) U–Pb

* Corresponding author.
E-mail address: d-satou@aist.go.jp (D. Sato).

http://dx.doi.org/10.1016/j.jvolgeores.2015.11.014

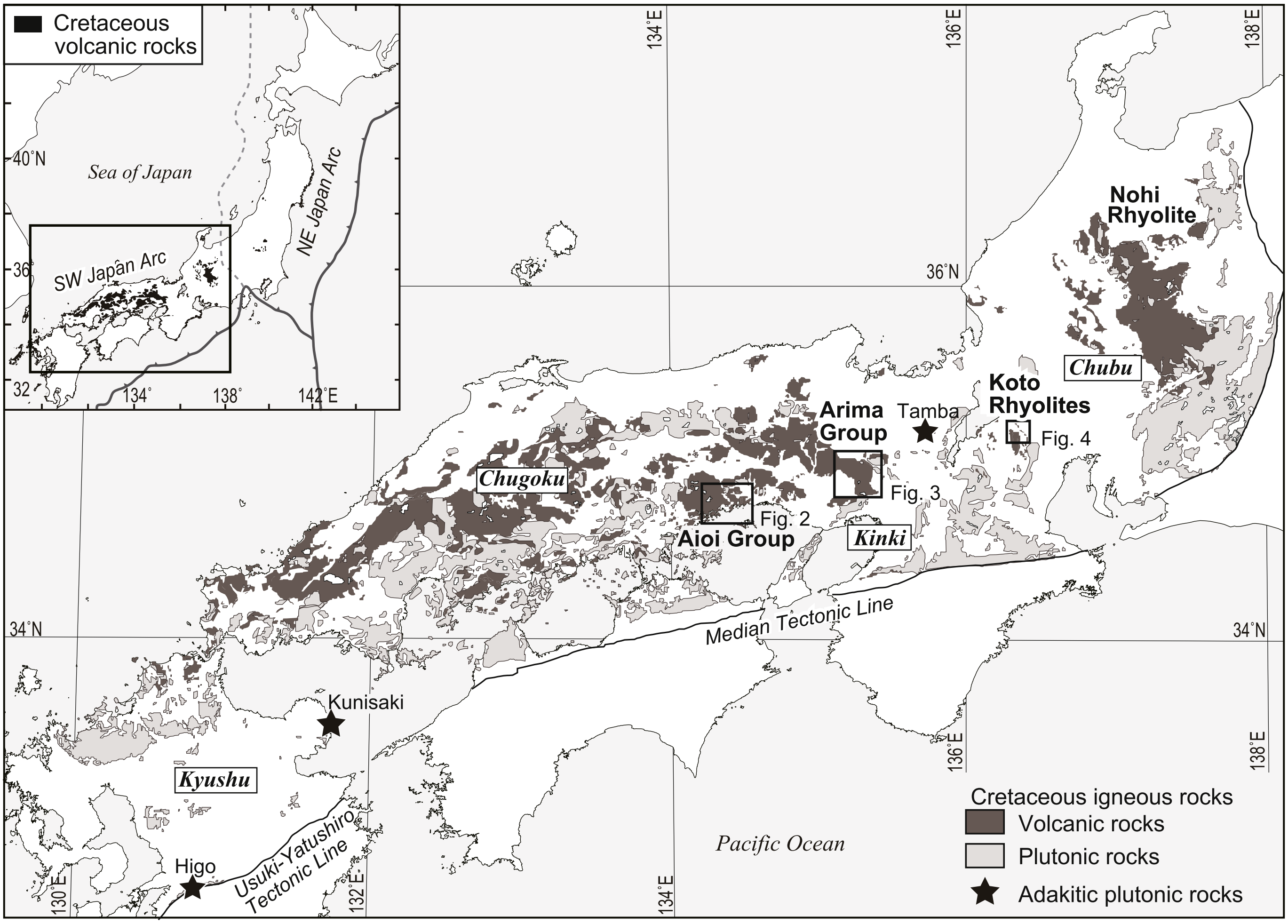

Fig. 1. Distribution of Cretaceous igneous rocks in southwest Japan (modified from Wakita et al., 2009).

zircon ages for individual pyroclastic flow deposits generated during Late Cretaceous caldera-forming eruptions in the Kinki district. These data enable the clarification of the timing of individual volcanic events. The closure temperature of the zircon U–Pb system is significantly higher (>900 °C; Cherniak and Watson, 2000) than those of the K–Ar biotite (280–345 °C; Harrison et al., 1985) and FT (240 °C; Hurford, 1986) systems. Although previous research has reported zircon U–Pb ages for Cretaceous granitoids in southwest Japan (e.g., Sakashima et al., 2003; Nakajima et al., 2004), the volcanic rocks in this region have not been dated using this method. The zircon U–Pb dates obtained during this study are generally from pyroclastic flow deposits collected from three volcanic groups in the Kinki district, namely the Aioi Group, the Arima Group, and the Koto Rhyolites (Fig. 1). We use these data to determine the timing of the Late Cretaceous ignimbrite flare-up within this arc.

2. Geological setting

The Kinki district is dominated by Permian to Jurassic terranes, Early Cretaceous sediments along with tuff and pyroclastic rocks, Cretaceous volcanic and plutonic rocks, and Paleogene to Quaternary sediments. Three Permian to Jurassic terranes are recognized based on geotectonic criteria: ophiolite rocks and Permian to Triassic marine sedimentary rocks of the Maizuru terrane (e.g., Ichikawa, 1990), Permian accretionary sedimentary complexes of the Ultra–Tamba terrane, and Jurassic accretionary sedimentary complexes of the Mino–Tamba terrane. Late Cretaceous volcanic rocks unconformably overlie and are often in fault and/or ring dike contact with Permian to Jurassic terranes. These volcanic rocks are divided into the Aioi, Ikuno, and Arima groups, and the Koto Rhyolites (Fig. 1). Previous research has indicated that Late Cretaceous volcanic rocks in this area are dominated by pyroclastic flow deposits related to caldera-forming events (e.g., Nishikawa et al., 1983; Ozaki and Matsuura, 1988; Yamamoto, 2003). The geology of each of these groups is summarized in the following sections.

2.1. Aioi Group

The Aioi Group consists mainly of pyroclastic flow deposits with minor amounts of lava and lacustrine deposits and crops out within the western area of the Kinki district (Fig. 1). These volcanic rocks fill depressions that are interpreted as calderas. The 40 × 50 km the western section of the Kinki district includes over 20 eroded calderas of <25 km in diameter (Yamamoto, 2003; Sato et al., in press). The calderas are commonly intruded by felsic dikes, from a few to a dozen meters in width, along boundaries between the caldera-fill deposits and surrounding basement rocks (Sato et al., in press). The southwestern part of the Aioi Group is divided into at least eight formations (from west to east): the Wake, Hinase, Une, Ako, Wakasano, Gomyo, Murotsu, and Iwami formations (Ishihara and Imaoka, 1999; Sato et al., in press) (Fig. 2). Each formation crops out over a limited area and sometimes show caldera depression structures. Pyroclastic flow deposits in the Wake Formation (15 km in diameter of preserved caldera fill) and the Ako Formation (21 km × 14 km in size) are interbedded with debris avalanche deposits in the form of caldera collapse breccias. The debris avalanche deposits in these formations consist of basement rocks with a wide variety of block sizes from a few centimeters to a dozen meters in diameter, and the matrix comprises the same materials but of finer

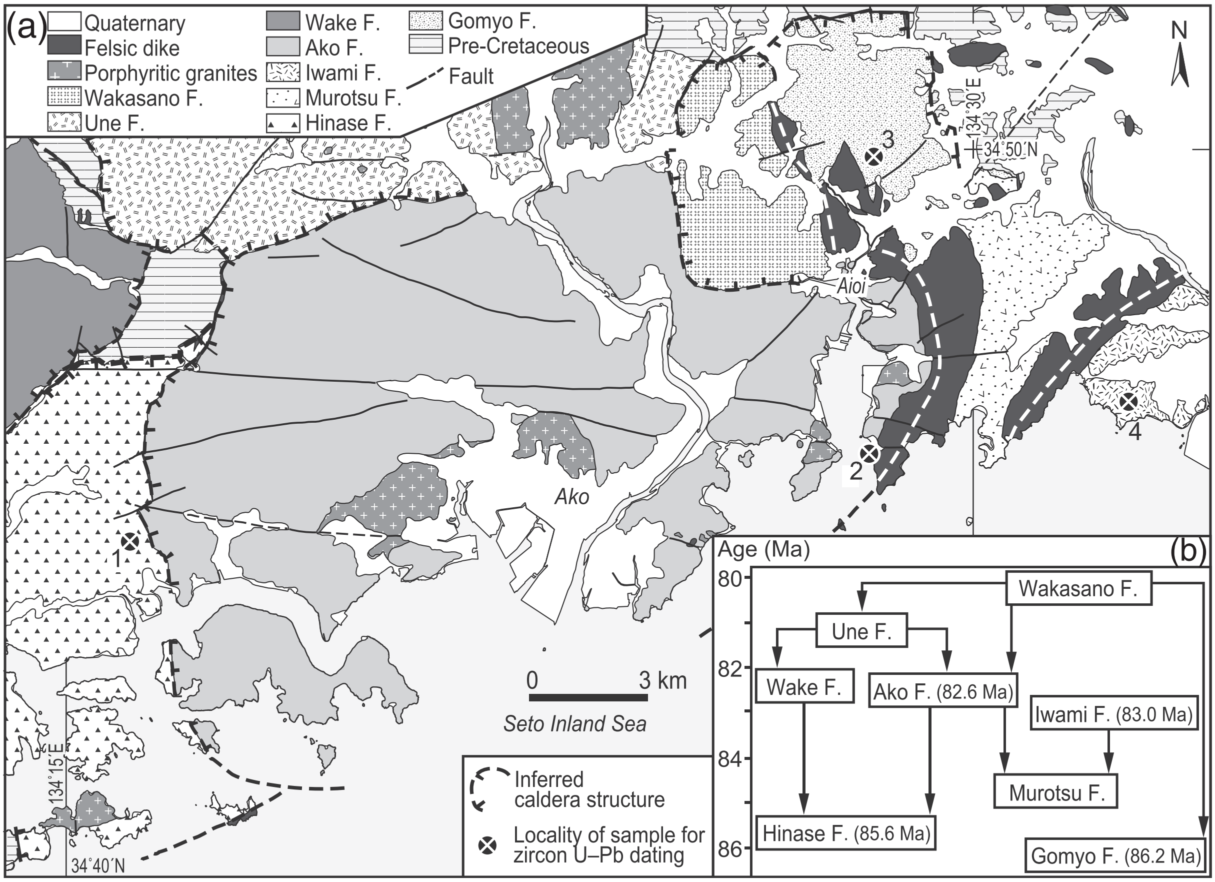

Fig. 2. Distribution of and stratigraphic relationships between volcanic formations in the southwestern Aioi Group. (a) Map showing the distribution of volcanic formations, adapted from Sato et al. (in press). 1 = sample from the Hinase Formation (BAK02), 2 = sample from the Ako Formation (BAK01), 3 = sample from the Gomyo Formation (BAK04), 4 = sample from the Iwami Formation (BAK03). (b) Stratigraphic relationship between volcanic formations in the study area; arrows indicate unconformable contacts visible in the field. The ages shown in the figure are U–Pb ages of the present study. F = formation.

grain size. The Ako Formation overlies the Hinase and Murotsu formations and includes lithic fragments derived from these formations and pre-Cretaceous rocks. The Hinase Formation (23 × 13 km), the Une Formation (18 × >6 km), and the Ako Formation were intruded by Late Cretaceous porphyritic plutonic rocks and underwent contact thermal metamorphism (Sato et al., in press).

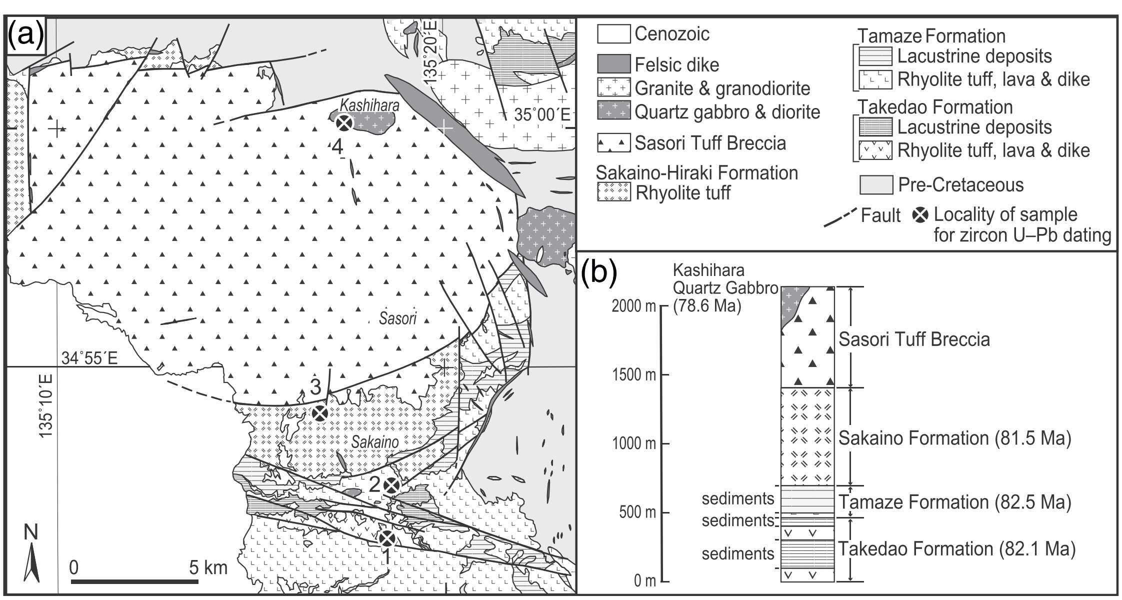

Fig. 3. Geological map and stratigraphic relationships of the Arima Group, adapted from Matsuura et al. (1995). (a) Geological map: 1 = sample from the Takedao Formation (HRN2), 2 = sample from the Tamaze Formation (HRN90A), 3 = sample from the Sakaino Formation (HRN14), 4 = sample from the Kashihara Quartz Gabbro (SON152). (b) Stratigraphic relationships of the Arima Group. Ages shown are U–Pb ages obtained during this study.

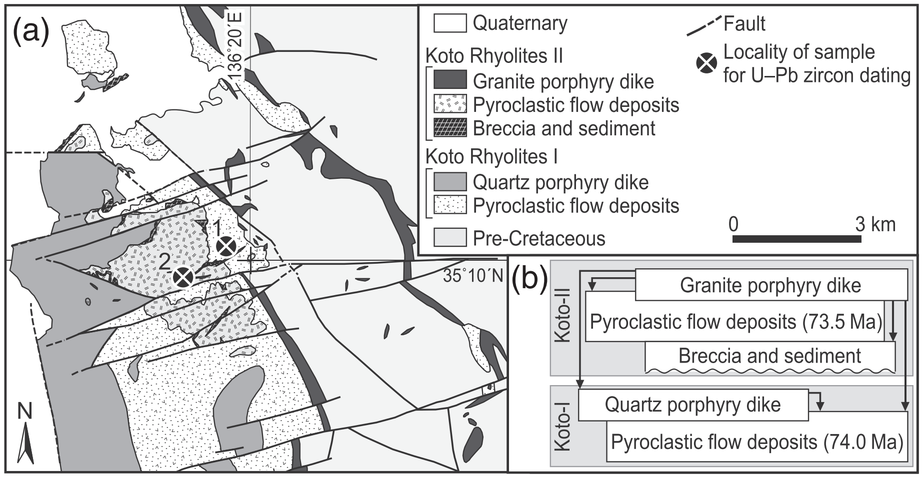

Fig. 4. Geological map and stratigraphy of the Koto Rhyolites, adapted from Harayama et al. (1989). (a) Geological map; 1 = sample from the Koto Rhyolites I (HK18LW), 2 = sample from the Koto Rhyolites II (KT43). (b) Stratigraphic relationships of the Koto Rhyolites. Arrows indicate unconformable contacts visible in the field and ages are U–Pb ages obtained during this study.

2.2. Arima Group

The Arima Group consists of pyroclastic flow deposits, lavas, and non-marine clastic sediments, and crops out within the central part of the Kinki district (Kasama and Yoshida, 1976; Matsuura et al., 1995) (Figs. 1 and 3). Late Cretaceous granitoids and dikes in this area intrude pre-Cretaceous rocks and the Arima Group. The southern area of the group consists of large-scale pyroclastic flow deposits generated during the formation of the Sasori Cauldron (19 × 14 km in size). The Arima Group is stratigraphically divided into four units (in ascending order): the Takedao, Tamaze, and Sakaino–Hiraki formations, and the Sasori Tuff Breccia. All of these formations are rhyolitic and are conformable, with a total thickness of ~2000 m. The Sasori Tuff Breccia is generally surrounded by polygonal faults associated with megabreccias (1–120 m in diameter) that were generated during caldera collapse, a process that occurred during or immediately after the eruption of a large volume of pyroclastic flow deposits that formed the Sakaino–Hiraki Formation (Matsuura et al., 1995).

2.3. Koto Rhyolites

The Koto Rhyolites consist of pyroclastic flow deposits and comagmatic porphyritic dikes that crop out within the eastern Kinki district (Mimura et al., 1976; Harayama et al., 1989) (Figs. 1 and 4). Cretaceous granitoids also crop out in a circular pattern surrounding the Koto Rhyolites. These rhyolites are remnants of a 30-km-diameter composite caldera (the Koto Cauldron) that is surrounded by two arcuate dikes (Nishikawa et al., 1983). The Koto Rhyolites are divided into an older unit (Koto Rhyolites I) that consists of dacite to rhyolite welded tuffs and porphyritic quartz dikes, and a younger unit (Koto Rhyolites II), which unconformably overlies the Koto Rhyolites I unit and consists of (from base to top) thin lacustrine sediments, debris avalanche deposits, rhyolite pumice tuffs, porphyritic granites, and pyroclastic dikes. Volcanic rocks from the older and younger units yield Rb–Sr whole rock isochron ages of 94.7 ± 19.6 Ma (Sawada et al., 1994) and 75.8 ± 2.4 Ma (Seki, 1978), respectively. These Rb–Sr isochron ages suggest that igneous activity occurred during three separate stages: Stage 1 activity formed the Koto Rhyolites I unit and associated older granitoids (97–95 Ma), Stage 2 activity formed the Koto Rhyolites II unit and younger granitoids (80–76 Ma), and Stage 3 activity saw the intrusion of dikes along the ring fracture zones until 66 Ma (Sawada et al., 1994).

3. LA–ICP–MS U–Pb geochronology

3.1. Samples

The samples used for U–Pb dating are zircons derived from the Aioi and Arima groups and the Koto Rhyolites. Zircons were separated from samples of four pyroclastic flow deposits from the Aioi Group (from the Hinase, Ako, Gomyo, and Iwami formations), and three pyroclastic flow deposits (from the Takedao, Tamaze, and Sakaino formations), and one post-caldera intrusion (the Kashihara Quartz Gabbro; Tainosho et al., 1983) from the Arima Group. Samples of two pyroclastic flow deposits

Table 1
Sample descriptions.

Sample	Location	Lithology	U–Pb age (Ma)
Aioi Group			
BAK01 (Ako Formation)	34°45′52″N, 134°28′18″E	Rhyolite welded vitric lapilli tuff	82.6 ± 0.8
BAK03 (Iwami Formation)	34°46′36″N, 134°32′33″E	Rhyolite welded crystal tuff	83.0 ± 0.5
BAK02 (Hinase Formation)	34°44′32″N, 134°16′16″E	Rhyolite welded crystal lapilli tuff	85.6 ± 0.6
BAK04 (Gomyo Formation)	34°49′52″N, 134°28′20″E	Dacite welded crystal tuff	86.2 ± 0.4
Kashihara Quartz Gabbro			
SON152/GSJ R63024	35°00′11″N, 135°17′11″E	Quartz diorite	78.6 ± 0.5
Arima Group			
HRN14/GSJ R62968 (Sakaino Formation)	34°54′04″N, 135°16′48″E	Rhyolite welded vitric crystal tuff	81.5 ± 0.7
HRN90A/GSJ R62889 (Tamaze Formation)	34°52′30″N, 135°18′35″E	Rhyolite welded crystal vitric lapilli tuff	82.5 ± 0.6
HRN2/GSJ R62817 (Takedao Formation)	34°51′21″N, 135°18′28″E	Rhyolite welded vitric crystal tuff	82.1 ± 0.5
Koto Rhyolites			
KT43/GSJ R44577 (Koto Rhyolites II)	35°09′49″N, 136°18′59″E	Rhyolite welded tuff	73.5 ± 0.6
HK18LW/GSJ R44575 (Koto Rhyolites I)	35°10′07″N, 136°19′36″E	Rhyolite welded tuff	74.0 ± 0.4

Table 2
Instrumentation and operational conditions used during LA–ICP–MS analyses.

Laser ablation
Model: New Wave Research NWR193
Laser type (wave length): Excimer ArF (193 nm)
Energy density: 2–3 J/cm^2
Crater size: 20 μm
Ablation pit depth: 6 μm pit depth
Repetition rate: 8–10 Hz
Carrier gas: He
ICP–MS
Model: Nu instruments AttoM
ICP–MS type: magnetic sector field
Forward power: 1300 W
Carrier gas: Ar
Ar gas flow rate: 0.9 L min^{-1}
He gas flow rate: 0.6 L min^{-1}
Scanning mode: Deflector jump
Data acquisition protocol: Batch
Integration time: 8 s
Monitor isotopes: ^{202}Hg, ^{204}Pb, ^{206}Pb, ^{207}Pb, ^{208}Pb, ^{232}Th, ^{238}U
Primary standard: 91500[1]
Secondary standard: OD-3[2,3]

1, Wiedenbeck et al. (1995); 2, Iwano et al. (2012); 3, Iwano et al. (2013)

from the Koto Rhyolites (from Koto Rhyolites I and II) were also analyzed. The sample locations within the Aioi Group, the Arima Group, and the Koto Rhyolites are shown in Figs. 2, 3, and 4, respectively, and details of sample locations and lithologies are provided in Table 1. The volcanic rocks range from dacite to rhyolite welded tuffs, all of which contain abundant zircons. The majority of these samples have undergone minor hydrothermal alteration, leading to the partial replacement of mafic silicates by chlorite and other secondary minerals. These units locally contain foreign lithic fragments, but the samples analyzed during this study were specifically selected to be as free of these fragments as possible. The Kashihara Quartz Gabbro intrudes the Sasori Tuff Breccia at the top of the Arima Group and comprises fine- to medium-grained quartz gabbro to quartz diorite with pyroxene phenocrysts that have been partly replaced by actinolite.

3.2. Analytical techniques

In situ U–Pb analyses were undertaken at the Kyoto Fission-Track Co., Ltd., Kyoto, Japan, using zircons separated from 10 samples (each 0.15–0.30 kg) using standard crushing, sieving, water-based panning, magnetic separation, and heavy liquid techniques. After separation, the zircons were mounted within PFA-Teflon sheets and polished. This analysis used an AttoM high-resolution double-focusing ICP–MS (Nu instruments, Wrexham, UK) combined with a NWR-193 laser-ablation system (ESI, Portland, USA) equipped with a 193 nm ArF Excimer laser at the Department of Geology and Mineralogy, Kyoto University, Japan (Table 2). Helium gas was used as the carrier gas inside the ablation cell and was mixed with argon gas before entering the ICP–MS. These analyses used a 20 μm diameter laser-ablation spot with a 6 μm pit depth, and U–Pb ratios were normalized using replicate analyses of a Nancy 91500 standard zircon (Wiedenbeck et al., 1995).

Cathodoluminescence (CL) imaging was used to determine internal zonation patterns within zircons. CL images were obtained using a JEOL JSM-6610LV scanning electron microscope (SEM) at the Geological Survey of Japan (GSJ, Tsukuba, Japan). Representative CL images of the zircons analyzed in this study are shown in Fig. 5.

3.3. Results

The zircon U–Pb data are summarized in Supplementary Tables 1–3. Tera–Wasserburg U–Pb zircon concordia diagrams for the Aioi Group, the Arima Group, and the Koto Rhyolites are shown in Fig. 6, with all uncertainties reported at the 2σ level. The precision of the ^{207}Pb/^{235}U measurements is generally poorer than that of the ^{206}Pb/^{238}U measurements; thus, the igneous ages used in this study are weighted mean ^{238}U–^{206}Pb ages. However, use of only ^{238}U–^{206}Pb ages can be erroneous if the U–Pb system is not closed, so this possibility was evaluated by examining the concordance of the ^{238}U–^{206}Pb and ^{235}U–^{207}Pb ages (e.g., Iwano et al., 2013). Discordant data show a disagreement between the ^{238}U–^{206}Pb and ^{235}U–^{207}Pb ages within the 2σ error and were therefore excluded from the weighted mean calculation and later discussion. The zircons are generally 50–200 μm in size, euhedral, transparent, and light brownish in color. The CL images reveal oscillatory zoning and characteristics that are typical of zircons with a magmatic origin (Fig. 5).

Samples from the Hinase Formation (BAK02; rhyolite welded crystal lapilli tuff), the Ako Formation (BAK01; rhyolite welded vitric lapilli tuff), the Gomyo Formation (BAK04; biotite–hornblende dacite welded crystal tuff), and the Iwami Formation (BAK03; biotite–hornblende rhyolite welded crystal tuff) within the Aioi Group yield ages of 85.6 ± 0.6 Ma (n = 24/30, MSWD = 1.37), 82.6 ± 0.8 Ma (n = 15/15, MSWD = 1.23), 86.2 ± 0.4 Ma (n = 23/30, MSWD = 2.25), and 83.0 ± 0.5 Ma (n = 27/30, MSWD = 2.02), respectively, all of which are consistent with observed stratigraphic relationships. These ages of adjacent formations (i.e., the Hinase–Ako–Gomyo formations) are not within error of each other.

Samples from the Takedao Formation (HRN2/GSJ R62817; biotite rhyolite welded vitric crystal tuff), the Tamaze Formation (HRN90A/GSJ R62889; biotite rhyolite welded crystal vitric lapilli tuff), and the Sakaino Formation (HRN14/GSJ R62968; hornblende-bearing biotite rhyolite welded vitric crystal tuff) within the Arima Group yield ages of 82.1 ± 0.5 Ma (n = 29/30, MSWD = 1.66), 82.5 ± 0.6 Ma (n = 30/30, MSWD = 1.04), and 81.5 ± 0.7 Ma (n = 29/30, MSWD = 0.59), respectively. A sample from the Kashihara Quartz Gabbro (SON152/GSJ R63024; medium-grained biotite–orthopyroxene–hornblende–quartz diorite) that intrudes the Sasori Tuff Breccia (i.e., the Sasori Cauldron) yields an age of 78.6 ± 0.5 Ma (n = 29/30, MSWD = 2.23). These ages of volcanic rocks in the Arima Group are not consistent with observed stratigraphic

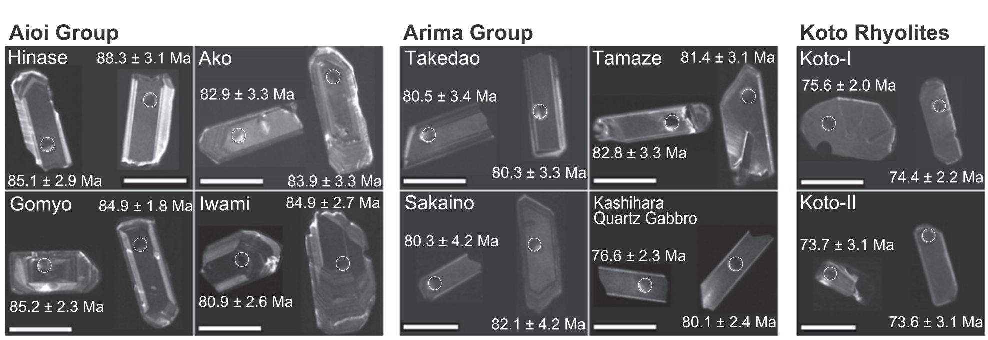

Fig. 5. Representative CL images of zircons separated from samples analyzed during this study. Numbers next to analytical spots (20 μm diameter) indicate the age of each analysis. Scale bars are 100 μm.

relationships but are all within error of each other. However, the Kashihara Quartz Gabbro records an apparent temporal gap in magmatism between 81 and 78 Ma, indicating that this intrusion occurred a significant time after the formation of the Arima Group.

Samples from the Koto Rhyolites I unit (HK18LW/GSJ R44575; pyroxene-bearing hornblende–biotite rhyolite welded tuff) and II unit (KT 43/GSJ R44577; biotite rhyolite welded tuff) yield ages of 74.0 ± 0.4 Ma (n = 29/30, MSWD = 2.90) and 73.5 ± 0.6 Ma (n = 27/31, MSWD = 2.48), respectively. These ages are consistent with observed stratigraphic relationships and are within error of each other.

4. Discussion

The closure temperature of the zircon U–Pb system (>900 °C) is higher than the crystallization temperature of zircon (700–850 °C; e.g., Harrison et al., 2007; Boehnke et al., 2013), so the granitoid U–Pb zircon ages in this study indicate the timing of granitoid emplacement rather than zircon crystallization. Determining the timing of emplacement of granitoid magmas requires knowledge of the cooling history of an intrusion using other radiometric ages. In contrast, volcanic rocks generally show little difference in the timing of zircon crystallization and

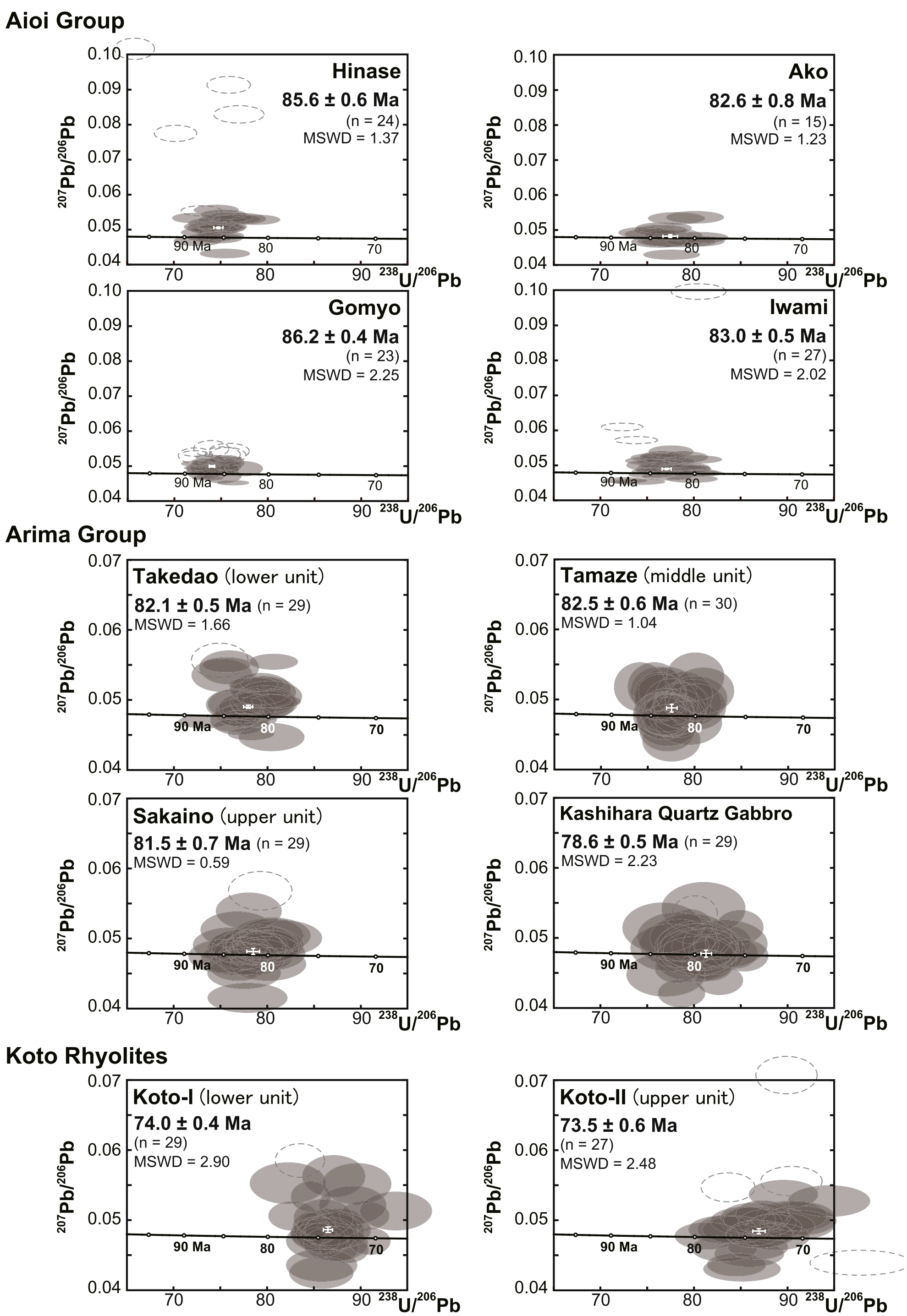

Fig. 6. Tera–Wasserburg diagrams for zircons analyzed during this study. Dashed circles indicate discordant analyses, error ellipses represent 2σ uncertainties for each analysis, error bars indicate weighted mean ^{238}U–^{206}Pb ages (2σ), and n = number of data points.

eruption ages. Crystal storage time is estimated by subtracting the age of the last eruption event from the zircon ages in the volcanic rocks. Sano et al. (2002) reported a zircon U–Pb isochron age of 90 ka from pyroclastic flow deposits that formed during the 1991 Unzen volcano eruption in the Nagasaki area of southwest Japan, suggesting that this age represents the timing of magma residence in a shallow reservoir before the eruption. Tucker et al. (2013) reported that crystal storage time of 48 ka from volcanic rocks in the Tibetan Plateau provide by high-spatial resolution U–Th disequilibrium dating methods. This indicates that the zircon U–Pb age of volcanic rocks is representative of the eruption age of such rocks, as the latter is generally within the 2σ uncertainty (i.e., several hundred thousand years) of the former. Although zircons within pyroclastic flow deposits are likely to include older zircons, the U–Pb zircon data presented here indicate significant differences between the ages of individual formations and are consistent with observed stratigraphic relationships within the Aioi Group. As such, we consider these ages to represent the eruption ages of individual formations.

4.1. Late Cretaceous igneous activity in the Kinki district

The ages of individual units in the Aioi Group are distinct from those of adjacent units (i.e., the age differences are greater than the analytical error). This suggests that the Aioi Group formed as a result of multiple Late Cretaceous caldera-forming eruptions that occurred at intervals of around 1 Myr. This scenario is similar to that in the Aizu region of the northeast Japan arc, where six large Late Miocene to Quaternary calderas, all of which are >10 km in diameter, erupted a total of six times over 7 Myr at intervals of 1–2 Myr (Yamamoto, 1992, 2011). This eruption interval is comparable to the age differences between the Gomyo, Hinase, Murotsu, Iwami, and Ako formations within the southwestern Aioi Group, where these formations represent four eruptions over a period of ca. 4 Myr (Fig. 2). As noted by Yamamoto (2003), this Late Cretaceous volcanism is thought to be similar in volume to the volcanism that occurred within the northeast Japan arc during the Late Miocene to Quaternary.

The U–Pb zircon ages obtained for the Arima Group range between 82.5 ± 0.6 Ma and 81.5 ± 0.7 Ma and are all the same within error. Matsuura et al. (1995) reported that the southern area of the Arima Group consists of large-scale pyroclastic flow deposits that were generated during caldera-formation events. This finding, combined with the data presented here, indicates that this igneous activity occurred at ca. 82 Ma and lasted for <1 Myr. In contrast, Imoto et al. (1991) reported that the Kashihara Quartz Gabbro, which intrudes the Sasori Tuff Breccia of the Arima Group, formed at the same time as the rhyolitic volcanic rocks. However, the zircon U–Pb age of the Kashihara Quartz Gabbro determined in this study is some 3 Myr younger than the ages of the Arima Group determined in this study (Figs. 6 and 7). This result, combined with the geology of the study area, suggests that the magmatism that formed the Kashihara Quartz Gabbro represents a separate event from that which formed the Arima Group units.

The zircon U–Pb ages of the Koto Rhyolites I and II units are both ca. 74 Ma, being the same within analytical error. The Koto Rhyolites I and II were formerly divided into two different caldera-forming stages that occurred at ca. 95 Ma (stage 1) and ca. 76 Ma (stage 2), based on whole-rock Rb–Sr isochron ages (e.g., Sawada et al., 1994). However, the oldest single concordant zircon U–Pb age for the Koto Rhyolites I unit is 77.9 ± 3.9 Ma (Supplementary Table 3). These data indicate that the igneous activity that formed the Koto Rhyolites represents the generation of a relatively short-lived (<1 Myr) composite caldera in a single caldera-forming event. This view is consistent with the geochemistry of the Koto Rhyolites I unit being different to that of older granitoids in this area, but similar to that of the Koto Rhyolites II unit as well as younger granitoids and arcuate dikes in the area (CRGGLB, 2008).

The ages obtained for the Aioi Group indicate the intervals and frequency of individual caldera-forming eruptions, whereas the ages from the Arima Group and the Koto Rhyolites show the duration of single caldera-forming events. Therefore, we suggest that individual Late Cretaceous caldera-forming eruptions occurred at interval of >1 Myr and lasted only a short period of time (<1 Myr).

4.2. Timing of the Cretaceous ignimbrite flare-up

Fig. 8 shows a compilation of ages for samples from the Kyushu and Chubu districts of Japan obtained using methods with relatively high closure temperatures; i.e., U–Pb zircon, CHIME zircon, monazite, and allanite ages. It should be noted that the ages of high-Mg volcanic rocks in this area are K–Ar ages, because no U–Pb or CHIME ages for these rocks have been obtained. The oldest ages for I-type granites in the Kyushu district center on ca. 110 Ma (Fig. 8). The ages of high-Mg and adakitic igneous rocks have been reported from the Kyushu district (113–109 Ma: Tobe, 2006; Tsutsumi et al., 2012), the Chugoku district (107–103 Ma: Imaoka et al., 1993; Matsuura, 1998), the Kinki district (109–99 Ma: Kimura and Kiji, 1993; Imaoka et al., 2014), and the Chubu district (99–97 Ma: Tanase et al., 1994; Yamada et al., 2001). These age data indicate that high-Mg and adakitic activity that took place have a range between 113 and 97 Ma and began at about the

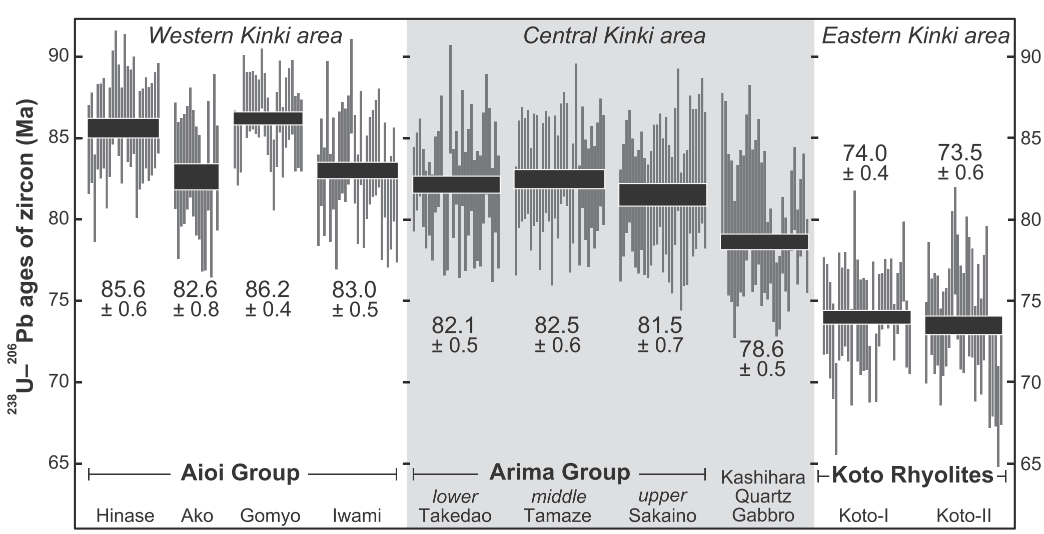

Fig. 7. Distribution of zircon U–Pb ages obtained during this study, excluding any discordant data. Vertical bars indicate individual U–Pb ages and associated uncertainties, with weighted mean ages shown as horizontal bars with errors represented by the heights of individual horizontal bars. All error bars are 2σ.

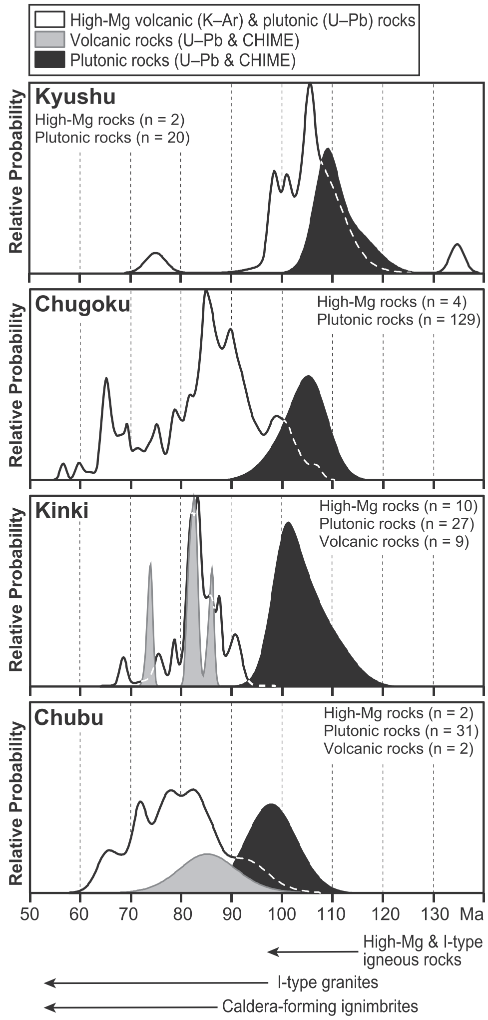

Fig. 8. Relative probability diagram of U–Pb and CHIME ages for plutonic rocks and ignimbrites, and K–Ar ages for high-Mg volcanic rocks in southwest Japan. Data from a compilation by Imaoka et al. (1993), Kimura and Kiji (1993), Tanase et al. (1994), Herzig et al. (1998), Matsuura (1998), Suzuki and Adachi (1998), Suzuki et al. (1998), Watanabe et al. (2000), Takagi et al. (2001), Yamada et al. (2001), Sakashima et al. (2003), Nakajima et al. (2004), Tobe (2006), Fujii et al. (2008), Ito et al. (2010, 2012), Adachi et al. (2012), Tiepolo et al. (2012), Tsutsumi et al. (2012), Ishihara and Tani (2013), Imaoka et al. (2014), Iida et al. (2015), and this study.

same time as I-type granite emplacement. Ages for caldera-forming volcanic rocks have been reported from the Kinki district (86–82 Ma; this study) and the Chubu district (86 ± 7 Ma and 85 ± 5 Ma; Suzuki et al., 1998) and the Chubu district yields the oldest volcanic unit in this area (the Nohi Rhyolite). The zircon U–Pb ages for pyroclastic flow deposits within the Aioi Group, Arima Group, and the Koto Rhyolites also span the time of formation of the Nohi Rhyolite unit, indicating that the oldest volcanic unit in the Kinki district formed at a similar time as the oldest volcanic units in the Chubu district. This finding indicates that caldera-forming eruptions across the Kinki district to the Chubu district began at ca. 90 Ma, and subsequent, this region is characterized by widespread silicic magmatism in the form of the volcano-plutonic complex activities.

Contrary to previous results obtained using conventional geochronological methods which suggested that the magmatism occurred gradually from 85 to 65 Ma with the caldera volcanoes erupting over long time intervals (the western Kinki district: Yamamoto, 2003; the Nohi area: Yamada and Koido, 2005), the U–Pb dates from this study show that the volcanism of the southwestern Aioi Group is concentrated within a short time period of 4 Myr. In the future, the combination of U–Pb zircon ages and geological data may enable the identification of individual volcanic units and further our understanding of volcanic activity in the Inner Zone of southwest Japan.

Acknowledgments

We thank Prof. Harayama of Shinshu University, Japan, and Dr. Sumii of the Geological Survey of Japan (GSJ) for providing some of the samples used during this study. We also sincerely thank Drs. Tohru Danhara and Hideki Iwano of Kyoto Fission-Track Co., Ltd., for the U–Pb analyses and useful comments on an earlier version of the manuscript. The description of the geology of the Aioi Group is based on field data obtained during the GSJ 'Geology of the Banshu-Ako district' project. We would like to thank Prof. Lang Farmer from University of Colorado, USA, and an anonymous reviewer for their thoughtful comments and suggestions.

Appendix A. Supplementary data

Supplementary data to this article can be found online at http://dx.doi.org/10.1016/j.jvolgeores.2015.11.014.

References

Adachi, T., Osanai, Y., Nakano, N., Owada, M., 2012. LA–ICP–MS U–Pb zircon and FE-EPMA U–Th–Pb monazite dating of pelitic granulites from the Mt. Ukidake area, Sefuri Mountains, northern Kyushu. J. Geol. Soc. Jpn. 118, 39–52.

Boehnke, P., Watson, E.B., Trail, D., Harrison, T.M., Schmitt, A.K., 2013. Zircon saturation re-revisited. Chem. Geol. 315, 324–334.

Cherniak, D.J., Watson, E.B., 2000. Pb diffusion in zircon. Chem. Geol. 172, 5–24.

Collaborative Research Group for the Granites around Lake Biwa (CRGGLB), 2008. Formation of the Hiei Granite pluton and its geological implications for the Cretaceous felsic magmatism in southwest Japan. J. Geol. Soc. Jpn. 114, 53–69 (in Japanese with English abstract).

Fujii, M., Hayasaka, Y., Horie, K., 2008. Metamorphism and timing of the nappe mobement in the Asaji metamorphic area, eastern Kyushu. Jour. Geol. Soc. Japan 114, 127–140 (in Japanese with English abstract).

Harayama, S., Miyamura, M., Yoshida, F., Mimura, K., Kurimoto, C., 1989. Geology of the Gozaishoyama district. With Geological Sheet Map at 1:50,000, Geol. Surv. Japan 145 pp. (in Japanese with English abstract).

Harrison, T.M., Duncan, I., McDougall, I., 1985. Diffusion of ^{40}Ar in biotite: temperature, pressure and compositional effects. Geochim. Cosmochim. Acta 49, 2461–2468.

Harrison, T.M., Watson, E.B., Aikman, A.B., 2007. Temperature spectra of zircon crystallization in plutonic rocks. Geology 35, 635–638.

Herzig, C.T., Kimbrough, D.L., Tainosho, Y., Kagami, H., Iizumi, S., Hayasaka, Y., 1998. Late Cretaceous U/Pb zircon ages and Precambrian crustal inheritance in Ryoke granitoids, Kinki and Yanai districts, Japan. Geochem. J. 32, 21–31.

Hurford, A.J., 1986. Cooling and uplift patterns in the Lepontine Alps South Central Switzerland and an age of vertical movement on the Insubric fault line. Contrib. Mineral. Petrol. 92, 413–427.

Ichikawa, K., 1990. Pre-Cretaceous terranes of Japan. In: Ichikawa, K. (Ed.), Pre-Cretaceous terranes of Japan. Publ. IGCP no. 224, Nippon Insatsu, Osaka, pp. 1–12.

Iida, K., Iwamori, H., Orihashi, Y., Park, T., Jwa, Y., Kwon, S.T., Danhara, T., Iwano, H., 2015. Tectonic reconstruction of batholith formation based on the spatiotemporal distribution of Cretaceous–Paleogene granitic rocks in southwestern Japan. Island Arc 24, 205–220.

Imaoka, T., Nakajima, T., Itaya, T., 1993. K–Ar ages of hornblendes in andesite and dacite from the Cretaceous Kanmon Group, Southwest Japan. J. Min. Petr. Econ. Geol. 88, 265–271.

Imaoka, T., Nakashima, K., Kamei, A., Itaya, T., Ohira, T., Nagashima, M., Kono, N., Kiji, M., 2014. Episodic magmatism at 105 Ma in the Kinki district, SW Japan: petrogenesis of Nb-rich lamprophyures and adakites, and geodynamic implications. Lithos 184–187, 105–131.

Imoto, N., Matsuura, H., Musashino, M., Shimizu, D., Ishida, S., 1991. Geology of the Sonobe district. With Geological Sheet Map at 1:50,000, Geol. Surv. Japan 68 pp. (in Japanese with English abstract).

Ishihara, S., Imaoka, T., 1999. A proposal of caldera-related genesis for the Roseki deposits in the Mitsuishi mining area, Southwest Japan. Resour. Geol. 49, 157–162.

Ishihara, S., Tani, K., 2013. Zircon age of granitoids hosting molybdenite–quartz vein deposits in the central Sanin Belt, Southwest Japan. Shigen-Chishitsu 63, 11–14 (in Japanese with English abstract).

Ito, H., Tamura, A., Morishita, T., Arai, S., 2010. Zircon U–Pb and fission-track ages of granitic rocks from the Nojima Fault and its vicinity: a new horizon for the LA–ICP–MS U–Pb dating method. Japan. Jour. Geol. Soc. Japan 116, 544–551 (in Japanese with English abstract).

Ito, H., Tamura, A., Morishita, T., Arai, S., 2012. Timing of some plutonic intrusions and tectonics in the Hida Mountain Range: an application LA–ICP–MS U–Pb dating on zircons. Jour. Geol. Soc. Japan 118, 449–456 (in Japanese with English abstract).

Iwano, H., Orihashi, Y., Danhara, T., Hirata, T., Ogasawara, M., 2012. Evaluation of fission-track and U–Pb double dating method for identical zircon grains: using homogeneous

zircon grains in Kawamoto Granodiorite in Shimane prefecture, Japan. Jour. Geol. Soc. Japan 118, 365–375 (in Japanese with English abstract).
Iwano, H., Orihashi, Y., Hirata, T., Ogasawara, M., Danhara, T., Horie, K., Hasebe, N., Sueoka, S., Tamura, A., Hayasaka, Y., Katsube, A., Ito, H., Tani, K., Kimura, J., Chang, Q., Kouchi, Y., Haruta, Y., Yamamoto, K., 2013. An inter-laboratory evaluation of OD–3 zircon for use as a secondary U–Pb dating standard. Island Arc 22, 382–394.
Kamei, A., Owada, M., Nagao, T., Shiraki, K., 2004. High-Mg diorite derived from sanukitic HMA magmas, Kyushu Island, southwest Japan arc: evidence from clinopyroxene and whole rock compositions. Lithos 75, 359–371.
Kasama, T., Yoshida, H., 1976. Volcanostratigraphy of the Late Mesozoic acid pyroclastic rocks of the Arima Group, Southwest Japan. J. Geosci. Osaka City Univ. 20, 19–42.
Kiji, M., Ozawa, H., Murata, M., 2000. Cretaceous adakitic Tamba granitoids in northern Kyoto, San'yo belt, Southwest Japan. Mineral. Petrol. Sci. 29, 136–149 (in Japanese with English abstract).
Kimura, K., Kiji, M., 1993. K–Ar ages of high-magnesian andesite and basalt sheets intruded into the Mino–Tamba belt, Southwest Japan. Jour. Geol. Soc. Japan 99, 205–208 (in Japanese).
Matsuura, H., 1998. K–Ar ages of the Early Cretaceous Shimonoseki Subgroup and the Kawara Granodiorite, Southwest Japan. J. Jpn. Assoc. Mineral. Petrol. Econ. Geol. 93, 307–312 (in Japanese with English abstract).
Matsuura, H., Kurimoto, C., Sangawa, A., Bunno, M., 1995. Geology of the Hirone district. With Geological Sheet Map at 1:50,000, Geol. Surv. Japan 110 pp. (in Japanese with English abstract).
Mimura, K., Katada, M., Kanaya, H., 1976. Igneous activity of the Koto Rhyolites in the Yatsuoyama district, southeast of Lake Biwa. Jour. Japan. Assoc. Mineral. Petrol. Econ. Geol. 71, 327–338 (in Japanese with English abstract).
Nakajima, T., Kamiyama, H., Williams, I.S., Tani, K., 2004. Mafic rocks from the Ryoke Belt, southwest Japan: implications for Cretaceous Ryoke/San-yo granitic magma genesis. Trans. R. Soc. Edinburgh: Earth Sci. 95, 249–263.
Nishikawa, K., Nishibori, T., Kohayakawa, T., Tajima, T., Joshima, M., Mimura, K., Katada, M., 1983. Koto Rhyolite and its igneous activity, Southwest Japan. J. Mineral. Petrol. Econ. Geol. 77, 51–64 (in Japanese with English abstract).
Ozaki, M., Matsuura, H., 1988. Geology of the Sanda district. With Geological Sheet Map at 1:50,000, Geol. Surv. Japan 93 pp. (in Japanese with English abstract).
Sakashima, T., Terada, K., Takeshita, T., Sano, Y., 2003. Large-scale displacement along the Median Tectonic Line, Japan: evidence from SHRIMP zircon U–Pb dating of granites and gneisses from the South Kitakami and paleo-Ryoke belts. J. Asian Earth Sci. 21, 1019–1039.
Sano, Y., Tsutsumi, Y., Terada, K., Kaneoka, I., 2002. Ion microprobe U–Pb dating of Quaternary zircon: implication for magma cooling and residence time. J. Volcanol. Geotherm. Res. 117, 285–296.
Sato, D., Yamamoto, T., Takagi, T., 2016. Geology of the Banshu-Ako district. Quadrangle Series, 1: 50,000, Geological Survey of Japan, AIST (in Japanese with English abstract), (in press).
Sawada, Y., Itaya, T., 1993. K–Ar ages of a Late Cretaceous granitic ring complex around southern Lake Biwa, Southwest Japan—cooling history of a huge cauldron. Jour. Geol. Soc. Japan 99, 975–990 (in Japanese with English abstract).
Sawada, Y., Kagami, H., Matsumoto, I., Sugii, S., Nakano, S., Collaborative Research Group for the Granites around Lake Biwa, 1994. A Cretaceous granitic ring complex and the Koto Cauldron around the southern part of Lake Biwa. J. Geol. Soc. Jpn. 100, 217–233 (in Japanese with English abstract).
Seki, T., 1978. Rb–Sr geochronology and petrogenesis of the Late Mesozoic igneous rocks in the inner zone of the southwestern part of Japan. Mem. Fac. Sci. Kyoto Univ., Ser. Geol. Mineral 45, 71–110.
Suzuki, K., Adachi, M., 1998. Denudation history of the high T/P Ryoke metamorphic belt, southwest Japan: constraints from CHIME monazite ages of gneisses and granitoids. J. Metamorph. Geol. 16, 23–37.
Suzuki, K., Nakazaki, M., Adachi, M., 1998. An 85 ± 5 Ma CHIME age for the Agigawa welded tuff sheet in the oldest volcanic sequence of the Nohi Rhyolite, central Japan. J. Earth Sci. Nagoya Univ. 45, 17–27.
Tainosho, Y., Nakajima, W., Nomura, A., Yasuo, T., Hirao, T., 1983. Acidic volcaniclastic and intrusive rocks in the environs of Hokusetu and Kenbi-san: a preliminary report. MAGMA 67, 57–62 (in Japanese).
Takagi, H., Tobe, E., Sakashima, T., Terada, K., 2001. Western extension of the Median Tectonic Line in Kyushu. Abstract of the 108th Annual Meeting of the Geological Society of Japan, p. 118 (in Japanese with English abstract).
Takahashi, M., 1983. Space-time distribution of late Mesozoic to early Cenozoic magmatism in East Asia and its tectonic implications. In: Hashimoto, M., Uyeda, S. (Eds.), Accretion Tectonics in the Circum-Pacific Ocean Regions. TERRAPUB, Tokyo pp, pp. 69–88.
Tanase, A., Yamada, N., Wakita, K., 1994. Hayashida Andesite –100 Ma calc-alkaline andesite in the uppermost reaches of Kuzuryu River, central Japan. Jour. Geol. Soc. Japan 100, 635–638 (in Japanese).
Tiepolo, M., Langone, A., Morishita, T., Yuhara, M., 2012. On the recycling of amphibole-rich ultramafic intrusive rocks in the arc crust: evidence from Shikanoshima Island (Kyushu, Japan). J. Petrol. 53, 1255–1285.
Tobe, E., 2006. Implications of isotopic ages of granites for the geotectonic evolution of middle Kyushu (Ph. D. thesis) The University of Waseda, Tokyo (61 pp.).
Tsutsumi, Y., Miyake, Y., Komatsu, T., 2012. LA–ICPMS zircon dating of basement rocks under the Himenoura Group on the Amakusa–kamijima Island, Kyushu, southwest Japan. Abstracts of the 2012 Annual Meeting of Japan Association Mineralogical Sciences, p. 185 (in Japanese with English abstract).
Tucker, R.T., Zou, H., Fan, Q., Schmitt, A.K., 2013. Ion microprobe dating of zircons from active Dayingshan volcano, Tengchong, SE Tibetan Plateau: time scales and nature of magma chamber storage. Lithos 172–173, 214–221.
Wakita, K., Igawa, T., Takarada, S., 2009. Seamless geological map of Japan at a scale of 1: 200,000 DVD Edition. Geol. Surv. Japan, AIST, Digital Geoscience Map G-16.
Watanabe, T., Ireland, T., Tainosho, Y., Nakai, Y., 2000. Zircon U–Pb sensitive high mass-resolution ion microprobe dating of granitoids in the Ryoke metamorphic belt, Kinki District, Southwest Japan. Island Arc 9, 55–63.
Wiedenbeck, M., Alle, P., Corfu, F., Griffin, W.L., Meier, M., Oberli, F., Von Quadt, A., Roddick, J.C., Spiegel, W., 1995. Three natural zircon standards for U–Th–Pb, Lu–Hf, trace element and REE analyses. Geostand. Newslett. 19, 1–23.
Yamada, N., Koido, Y., 2005. Nohi Rhyolite: distribution, basement rocks, ages and lithologic features. Monograph 53, 15–28 (in Japanese with English abstract).
Yamada, N., Takizawa, F., Tanase, A., Kawada, K., 2001. K–Ar ages of the Oyashirazu Formation: an evidence of about 100 Ma andesitic volcanism in the border area of Toyama and Niigata prefectures, central Japan. Earth Sci. (Chikyu Kagaku) 55, 113–118 (in Japanese).
Yamamoto, T., 1992. Chronology of the Late Miocene–Pleistocene caldera volcanoes in the Aizu district, Northeast Japan. Jour. Geol. Soc. Japan 98, 21–38 (in Japanese with English abstract).
Yamamoto, T., 2003. Lithofacies and eruption ages of Late Cretaceous caldera volcanoes in the Himeji–Yamasaki district, southwest Japan: implications for ancient large-scale felsic arc volcanism. Island Arc 12, 294–309.
Yamamoto, T., 2011. Origin of the sequential Shirakawa ignimbrite magmas from the Aizu caldera cluster, northeast Japan: evidence for renewal of magma system involving a crustal hot zone. J. Volcanol. Geotherm. Res. 204, 91–106.